

## Exploring the oxidative mechanisms of bitumen after laboratory short- and long-term ageing

Pipintakos, Georgios; Soenen, Hilde; Ching, H. Y. Vincent; Velde, Christophe Vande; Doorslaer, Sabine Van; Lemièrre, Filip; Varveri, Aikaterini; Van den bergh, Wim

**DOI**

[10.1016/j.conbuildmat.2021.123182](https://doi.org/10.1016/j.conbuildmat.2021.123182)

**Publication date**

2021

**Document Version**

Final published version

**Published in**

Construction and Building Materials

**Citation (APA)**

Pipintakos, G., Soenen, H., Ching, H. Y. V., Velde, C. V., Doorslaer, S. V., Lemièrre, F., Varveri, A., & Van den bergh, W. (2021). Exploring the oxidative mechanisms of bitumen after laboratory short- and long-term ageing. *Construction and Building Materials*, 289, 1-12. Article 123182. <https://doi.org/10.1016/j.conbuildmat.2021.123182>

**Important note**

To cite this publication, please use the final published version (if applicable). Please check the document version above.

**Copyright**

Other than for strictly personal use, it is not permitted to download, forward or distribute the text or part of it, without the consent of the author(s) and/or copyright holder(s), unless the work is under an open content license such as Creative Commons.

**Takedown policy**

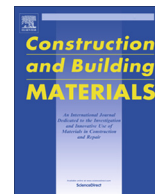
Please contact us and provide details if you believe this document breaches copyrights. We will remove access to the work immediately and investigate your claim.

***Green Open Access added to TU Delft Institutional Repository***

***'You share, we take care!' - Taverne project***

**<https://www.openaccess.nl/en/you-share-we-take-care>**

Otherwise as indicated in the copyright section: the publisher is the copyright holder of this work and the author uses the Dutch legislation to make this work public.



## Exploring the oxidative mechanisms of bitumen after laboratory short- and long-term ageing



Georgios Pipintakos<sup>a,\*</sup>, Hilde Soenen<sup>b</sup>, H.Y. Vincent Ching<sup>c</sup>, Christophe Vande Velde<sup>d</sup>, Sabine Van Doorslaer<sup>c</sup>, Filip Lemière<sup>e</sup>, Aikaterini Varveri<sup>f</sup>, Wim Van den bergh<sup>a</sup>

<sup>a</sup> University of Antwerp, EMIB Research Group, Groenenborgerlaan 171, Antwerp 2020, Belgium

<sup>b</sup> Nynas NV, Groenenborgerlaan 171, Antwerp 2020, Belgium

<sup>c</sup> University of Antwerp, BIMEF Research Group, Universiteitsplein 1, Wilrijk 2610, Belgium

<sup>d</sup> University of Antwerp, iPRACS Research Group, Groenenborgerlaan 171, Antwerp 2020, Belgium

<sup>e</sup> University of Antwerp, BAMS Research Group, Groenenborgerlaan 171, Antwerp 2020, Belgium

<sup>f</sup> Delft University of Technology, Pavement Engineering, Stevinweg 1, Delft 2628 CN, Netherlands

### HIGHLIGHTS

- The oxidative mechanisms in bitumen were studied after laboratory short- and long-term ageing.
- Three binders of varying crude source, distillation, performance and wax presence were investigated.
- <sup>1</sup>H NMR demonstrated slight changes in the relative proton distribution upon ageing.
- EPR supported an increase of organic carbon-centred radicals after short-term ageing.
- TOF-SIMS revealed an increase of SO<sub>x</sub>-, (OH)<sub>x</sub>-containing compounds because of ageing.

### ARTICLE INFO

#### Article history:

Received 5 January 2021

Received in revised form 5 March 2021

Accepted 25 March 2021

Available online 10 April 2021

#### Keywords:

Bitumen

EPR

<sup>1</sup>H NMR

TOF-SIMS

FTIR

Ageing

Oxidative mechanisms

### ABSTRACT

Understanding the fundamental mechanisms of oxidative ageing in bitumen is considered of paramount importance in order to take steps towards durable binders able to tackle distresses related to this phenomenon which deteriorates the asphalt performance. This paper focuses on the identification of the intermediate and final oxygenated products after short- and long-term laboratory ageing simulated with rolling thin-film oven testing (RTFOT) and pressurised ageing vessel (PAV) respectively. Three binders were investigated in this study, two originated from the same wax-free crude source, while the third was obtained from a different source, containing natural wax, and followed a different manufacturing process. Fourier-Transform Infrared (FTIR) spectroscopy demonstrated a clear increase of the sulfoxide and carbonyl functional groups upon ageing for all the binders independently of origin, manufacturing or performance. Electron Paramagnetic Resonance (EPR) spectroscopy showed an increase of the organic carbon-centred radicals after short-term ageing (RTFOT), whereas after PAV these radicals remained constant in the two wax-free binders originating from the same crude source, and even decreased for the third, waxy binder. Proton Nuclear Magnetic Resonance (<sup>1</sup>H NMR) spectroscopy reported differences in the relative distribution of protons between the binders in the unaged state, and similar minor changes after both ageing steps regardless of the binder's crude source and distillation. The results of Time-of-Flight Secondary Ion Mass Spectrometry (TOF-SIMS) revealed that SO<sub>x</sub>- and (OH)<sub>x</sub>-containing compounds are produced after the sequentially occurring short- and long-term ageing in both wax-free bitumens, whereas an almost constant behaviour of aliphatics after PAV ageing can be seen for the same bitumens. Finally, the strengths and weaknesses of each of these experimental techniques were reviewed and compared versus the obtained results and possible ageing mechanisms.

© 2021 Elsevier Ltd. All rights reserved.

\* Corresponding author.

E-mail address: [Georgios.Pipintakos@uantwerpen.be](mailto:Georgios.Pipintakos@uantwerpen.be) (G. Pipintakos).

## 1. Introduction

Bitumen is one of the main components of asphalt pavements and consists of a vast number of organic molecules [1]. Due to its organic constituents bitumen is prone to oxidation during exposure to mixing and environmental conditions [2]. Albeit other irreversible physicochemical processes take place in bitumen (volatilisation and condensation), oxidative ageing is considered of utmost importance since it generally deteriorates the pavement performance [3,4]. To date, a lot of studies have already demonstrated this negative impact of oxidative ageing resulting in the brittleness of bitumen responsible for several distresses in asphalt scale such as cracking and ravelling [5–8]. However, it should be noted that moderated ageing may indicate also positive effects in pavement if one is able to control it, *i.e.* by reducing severe deformations and rutting.

Since the chemical structure of bitumen is complex and also changes as a result of oxidative ageing, it has become apparent how crucial the understanding of bitumen chemistry is [9]. The bitumen's exact composition depends on the refinery process and the origin of crude oil, a fact that makes the determination of bitumen chemistry even more challenging [10,11]. Despite these difficulties, it has been proposed that the reaction mechanisms in each bitumen follow two-rate determining oxidation phases: the chemically distinct fast and slow phases [6,12,13]. Initiated by Petersen and his coworkers, recent literature confirmed experimentally the formation of organic carbon-centred radicals, which would be expected in a dual-sequential oxidation scheme [12,14]. The existence of free radicals will most likely provoke the chemical reactions resulting eventually in the formation of polar sulfoxides from non-polar sulfides and polar ketones (as well as anhydrides and carboxylic acids in smaller amounts) from benzylic carbon moieties [9].

Hitherto, isothermal reaction kinetic studies revealed also differences in the reaction rate and the formation of the two major oxidation products, namely carbonyls and sulfoxides [15]. Moreover, high temperatures, above 120 °C may cause thermal decomposition of the sulfoxides [13,16] and as such better insights into the sequential two-phase mechanism are needed since, in reality, the temperature varies between the different stages of the service life. It is important to note that during service life extreme temperatures greater than 80 °C are never reached, while the temperatures during the paving stages depend on the asphalt mixture application (hot, warm, cold).

It has long been speculated that certain oxidation products correlate well with the viscosity of bitumen [6,17]. Previous research highlighted additionally that the effect of temperature during the production stage, responsible for the short-term ageing, is more crucial for the intensity of the main oxidation products than the temperature during service life, associated with the long-term ageing of bitumen [18,19]. The effect of ageing time of each stage is considered also crucial for the end products and the bitumen's rheological behaviour. Moreover, to realistically capture the main products formed upon ageing as well as the role of intermediate products and organic radicals, one should go beyond isothermal kinetics. Ideally, taking also into account the effect of mineral fillers in the composition has been considered to be a more precise approximation of field ageing [20], although the interactions between the components yet remain to be understood.

In order to mimic in-situ changes of bitumen due to oxidation, a common practice is to utilise routine tests simulating the short- and long-term ageing. More specifically, the rolling thin film oven test (RTFOT) [21] followed by the pressurised ageing vessel (PAV) [22] are most commonly used to simulate the elevated temperature during production and paving and the weather conditions during use-life respectively. According to literature conditioning

in PAV of 20 h at a pressure of 2.1 MPa corresponds to 7–10 years of field ageing for base layers [23–25], where the exact equivalence depends on the bitumen and type of the asphalt mixture (dense, porous, etc.). However, controversy exists whether the high temperatures and pressure employed in artificial ageing can adequately capture the changes from a chemical perspective as the chemical mechanisms, in reality, may be somewhat different [9,26]. For example, the exposure to ultraviolet radiation or the incorporation of reactive oxygen species in the atmosphere can alter considerably the overall chemical routes or concentration of oxygenated products during ageing [27,28].

Of pragmatic importance is to examine whether the artificial ageing simulations, widely used in the asphalt sector, account for a fair correspondence with the ageing mechanisms reported previously in kinetic studies [12,15,29]. A fundamental understanding of bitumen oxidation is considered crucial for the implementation of the appropriate modifiers or rejuvenators when recycling and the reviewing of the protocols for artificial ageing, in order to adapt them in a controlled manner. Last but not least, taking steps towards the partial or complete prevention of oxidation in asphalt will bridge the gap between the depletion of an organic, non-renewable material, like bitumen, and a universal policy promoting long-lasting pavements and sustainability.

Given that the molecular interactions and chemical composition affect primarily the ability of molecules to flow and consequently the rheological behaviour of bitumen [4,30–32], an in-depth inspection of the underlying mechanisms after standardised simulations is thus considered more than crucial. This study aims primarily to identify the basic ageing compounds formed after artificial ageing. Specifically, the proposed approach employs advanced spectroscopy (FTIR, EPR, <sup>1</sup>H NMR and TOF-SIMS) in an attempt to capture the structural and chemical changes upon ageing with routine laboratory tests. This work aims finally at accounting for the effect of both the crude source, the binder's penetration grade and the distillation process on the mechanisms upon standardised ageing.

## 2. Materials and methods

### 2.1. Materials

The bituminous binders selected for this work vary with regard to the penetration grade, origin of the crude oil and refinery process. Bitumen A and B are straight-run binders, originating from the same acidic, wax-free crude with a penetration grade of 10/20 and 160/200 respectively. A third binder C of a different crude source with similar penetration to binder B was also examined, however, this binder was the result of a thermal cracking process (visbreaking) and it contained natural wax (crystallisable compounds). The wax presence was identified via Differential Scanning Calorimetry measurements and revealed a melting enthalpy of 9.6 J/g. The empirical properties of all binders are summarised in Table 1.

### 2.2. Ageing simulations

The oxidative ageing in the lab was simulated for the short term-ageing by the rolling thin film oven test (RTFOT) according to EN 12607-1 [21] and for the long-term ageing with the pressurised ageing vessel (PAV) according to EN 14769 [22]. Typically for RTFOT, 35 g of unaged virgin bitumen are placed in each bottle inside a rotating carousel for 75 min, where temperature and fresh air flow are set at 163 °C and 4 L/min. This test simulates the high temperatures occurring during the production and is linked with the initial fast-rate oxidation phase of a dual-sequential oxidation

**Table 1**  
Empirical properties of the bituminous binders in the unaged state.

| Material | Property                   | Binder |       |       | Test Method |
|----------|----------------------------|--------|-------|-------|-------------|
|          |                            | A      | B     | C     |             |
| Bitumen  | Penetration 25 °C (0.1 mm) | 16     | 189   | 190   | EN1426      |
|          | Softening point (°C)       | 61.1   | 37.5  | 39.2  | EN1427      |
|          | Penetration index, Ip      | -1.06  | -1.46 | -0.63 | EN12591     |
|          | Performance grade          | 76-16  | 52-28 | 52-22 | AASHTO MP 1 |

scheme. The PAV protocol, on the other hand, was followed for all the short-term aged samples after RTFOT, in an attempt to reproduce in a short period of time the effect of many years in the field. The PAV procedure requires 50 g of bitumen to be placed in pans inside a pressure chamber, which results in a thin film of bitumen able to be sufficiently aged. In the current study, the temperature was set at 100 °C with an air pressure of 2.1 MPa for a total duration of 20 h.

In order to simplify the nomenclature for each ageing state of the three binders, the following code ‘X-ageing state’ indicates the type of binder X (A, B or C) and the ageing state (Unaged, RTFOT or PAV). After applying the ageing conditions, appropriate samples were prepared for each spectroscopic technique described in the following subsection. For the ease of the reader, a graphical summary with the expected outcomes by each analysis is provided in Fig. 1.

2.3. Spectroscopic techniques

2.3.1. Attenuated total reflectance-Fourier transform infrared (ATR-FTIR)

For all the ageing states of each bitumen at least three individual samples were analysed using a Thermo Scientific Nicolet iS10 FTIR spectrometer equipped with an Attenuated Total Reflectance (ATR) fixture (diamond crystal) and a Smart Orbit Sampling Accessory. For the sample preparation, metal cans containing the bituminous materials were heated in an oven at 155 °C for 20 min. This time and temperature were found to be sufficient for all the used bitumens and ageing states to obtain a liquid sample which was afterwards stirred for 1 min and a single droplet was placed on the diamond FTIR crystal, after a background spectrum acquisition. The droplet was allowed to cool down for 5 min. The spectra were recorded as the average of 32 repetitive scans, at a resolution of 4 cm<sup>-1</sup>, in a wavenumber band ranging from 400 cm<sup>-1</sup> to 4000 cm<sup>-1</sup>. The analysis of the spectrum involves the calculation of band-areas in certain peaks from which chemical indices with regard to ageing of bitumen and its structural fingerprint can be derived. The reader is referred to the protocol given in Ref. [33] and to the calculation of the areas with their wavelength limits

and corresponding bond vibrations in Ref. [12]. The indices that can be extracted by making use of these areas are given in Eqs. (1)–(4). Example spectra of bitumen A in the three ageing states are given in Fig. 2.

$$\text{Sulfoxide index} = \frac{A_{1030}}{\sum^n A_n} \tag{1}$$

$$\text{Carbonyl index} = \frac{A_{1700}}{\sum^n A_n} \tag{2}$$

$$\text{Branched aliphatic index} = \frac{A_{1376}}{A_{1460} + A_{1376}} \tag{3}$$

$$\text{Aromaticity index} = \frac{A_{1600}}{\sum^n A_n} \tag{4}$$

where  $n = 724, 743, 814, 864, 1030, 1376, 1460, 1600, 1700, 2862, 2953$

2.3.2. Electron paramagnetic resonance (EPR)

For the identification of the organic radicals and metal ions, continuous-wave (CW) EPR spectra of the three binders in all the ageing states were acquired with a Bruker Elexsys E680 (X/W) spectrometer equipped with an ER 4102ST TE102 mode resonator at 9.75 GHz (X-band). Three replicates for each ageing state and each binder were placed inside propylene Eppendorf tubes and the exact masses were measured priorly in order to normalise the number of spins per gram for each detected paramagnetic component. It was found that all the recorded spectra include contributions of a vanadyl centre (VO<sup>2+</sup>,  $S = 1/2$ ) and an organic carbon-centred radical. The protocol described previously in Ref. [12] was followed here. Briefly, in a preliminary study the effects of power saturation were assessed and for all the subsequent measurements a microwave power of 0.5 mW, a centre magnetic field at 341 mT and sweep width of 20 mT, resolution of 2048 points, a modulation amplitude of 0.1 mT and a modulation frequency of 100 kHz over 2 scans, was selected. The spectra were next simulated with the EasySpin-6.0 module [34] in Matlab2018b from

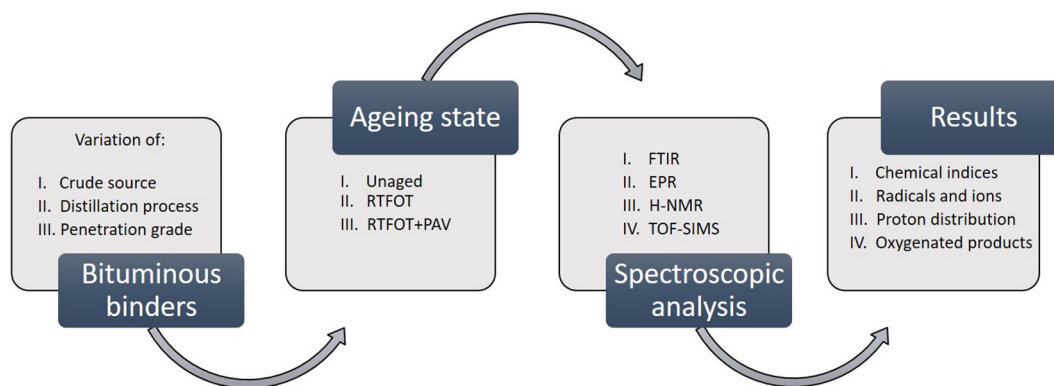


Fig. 1. Research methodology.

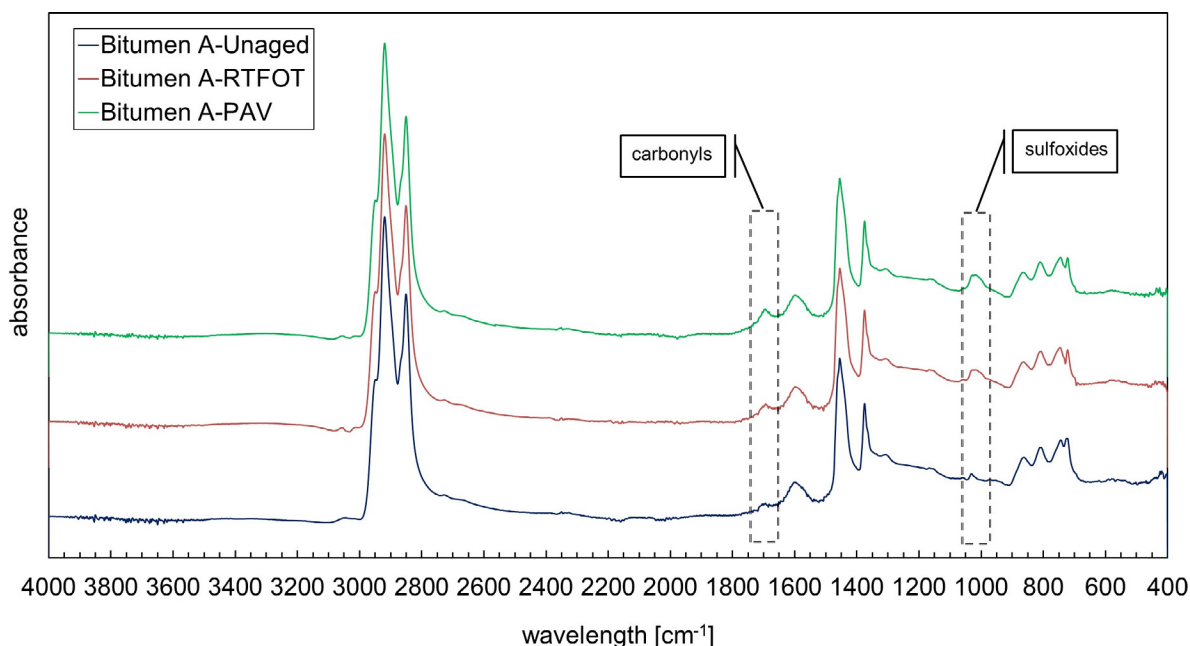


Fig. 2. Example of FTIR spectra in all the ageing states of bitumen A with the main oxygenated functional groups.

which the EPR parameters (given in Ref. [12]) of the two species and the relative amount of spins between them can be derived. The  $\text{VO}^{2+}$  centres were attributed to  $\text{VO}^{2+}$  porphyrin centres found in heavy crude oils [35,36] while the second signal was assigned to carbon-based organic radicals [37]. Quantification of the corresponding number of spins was obtained by comparison of the double integral of the spectra with standard curve derived using different concentrations of TEMPO (2,2,6,6-tetramethyl-1-piperidinyloxy) in toluene.

### 2.3.3. Proton nuclear magnetic resonance ( $^1\text{H}$ NMR)

$^1\text{H}$  NMR is a superior spectroscopic technique able to characterise the molecular structure of a material, even for a complex one, such as bitumen. It can assist with the characterisation of the relative amount of different types of aliphatic olefinic and aromatic protons in bitumen [38,39] and therefore can also be applied to capture the proton distribution upon ageing in bitumen. Data collection of all the bituminous binders at room temperature was conducted with a high-resolution liquid-state Bruker Avance III HD 400 MHz smart probe spectrometer (32 scans). Preliminary measurements with  $\text{CDCl}_3$  (deuterated chloroform) as solvent showed interference with the aromatic region signal of bitumen, while different concentrations of dissolution with 5 and 40 mg of bitumen showed a poor and an overloaded  $^1\text{H}$  NMR signal respectively. Therefore, about 20 mg of bitumen were dissolved in 650  $\mu\text{l}$  of deuterated tetrachloroethane ( $\text{C}_2\text{D}_2\text{Cl}_4$ ) inside borosilicate NMR tubes (ASTM Type 1 Class B glass) of diameter 5 mm and a wall thickness of 0.4 mm. To ensure an adequate dissolution of the solvent with the specimen all vials containing the dissolved samples were additionally placed inside an ultrasonic water bath before the  $^1\text{H}$  NMR analysis. The repeatability was provided by means of standard deviations. After the analysis, steps were first taken to accurately calibrate the starting chemical shift based on the difference of the residue solvent peak (6.00 ppm) with respect to TMS (tetramethylsilane) (0.00 ppm) [40]. The analysis of the results was performed in the MestreNova spectral analysing software following the integration of the typical proton chemical shift regions reported in [41], neglecting each time the protons associated to heteroatoms and the residue solvent at 6.00 ppm. The latter study

classifies a typical  $^1\text{H}$  NMR spectrum of bitumen in five main groups given in Table 2. Normalisation of all the integrated areas with the exact sample mass allows for a fair comparison of the relative percentage distribution of the different type of protons identified in bituminous samples. The normalised per mass areas were also inspected and same trends with the relative percentage distribution were followed, therefore the latter was chosen for the analysis of this study. Fig. 3 illustrates examples of spectra of bitumen A in all ageing states with the normalised per sample mass area integrations.

### 2.3.4. Time-of-flight secondary ion mass spectrometry (TOF-SIMS)

A TOF-SIMS IV spectrometer (ION-TOF GmbH) was utilised in this study, with the ultimate goal to unwrap the molecular structure of the products formed upon complete oxidation at the surface of bituminous samples. A bismuth liquid metal ion gun was used for bombarding the surface of bituminous samples with 25 keV  $\text{Bi}_3^+$  primary ions. The secondary ions emitted from the surface were separated based on the mass-to-charge ratio ( $m/z$ ) by the TOF analyser [42]. Mass spectra were recorded up to  $m/z$  1270. Charging of the sample was compensated using the electron flood gun. The instrument was controlled and data acquired by the IONVAC software (IonTOF). The data were processed using Surfcelab 7 (IonTOF).

Table 2  
Typical groups of protons in bitumen [41].

| Designation                      | Chemical shift range | Type of protons  | Major proton peak in this region |
|----------------------------------|----------------------|--|----------------------------------|
| $\text{H}_{\text{methyl}}$       | 0.5–1.0              | Aliphatic hydrogen on $\text{C}_\gamma$ and the $\text{CH}_3$ beyond the $\text{C}_\gamma$ to aromatic rings | Methyl                           |
| $\text{H}_{\text{methylene}}$    | 1.0–2.0              | Aliphatic hydrogen on $\text{C}_\beta$ and the $\text{CH}_2$ beyond the $\text{C}_\beta$ to aromatic rings   | Methylene                        |
| $\text{H}_{\alpha\text{-alkyl}}$ | 2.0–4.0              | Aliphatic hydrogen on $\text{C}_\alpha$ to aromatic rings  | –                                |
| $\text{H}_{\text{olefinic}}$     | 4.0–6.0              | Olefinic hydrogen  | –                                |
| $\text{H}_{\text{aromatic}}$     | 6.0–9.0              | Aromatic hydrogen  | –                                |

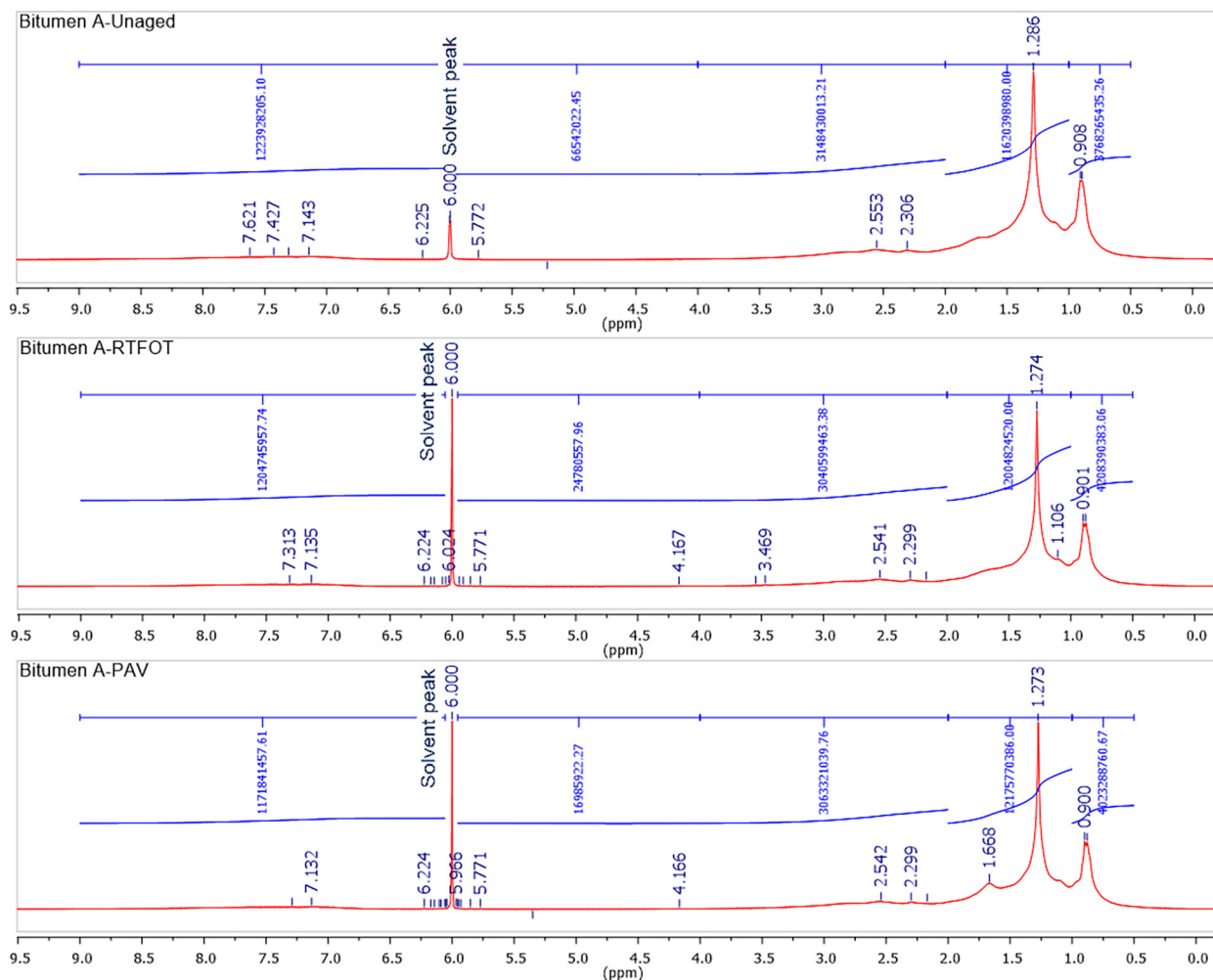


Fig. 3. Example of  $^1\text{H}$  NMR spectra in all the ageing states of bitumen A with their main proton peaks.

Following the procedure for conditioning of the samples described in Refs. [12,43] the temperature of the sample in the ion source was maintained between  $-50$  and  $-80$  °C using liquid nitrogen, in order to avoid diffusion/segregation in the vacuum system. Silicon wafers of dimensions  $10\text{ mm} \times 10\text{ mm}$  were used as substrates for the three bituminous binders in both the unaged and PAV ageing condition. Spectra of positive and negative ions were recorded at three different spots per sample in analysis areas of  $500\text{ }\mu\text{m} \times 500\text{ }\mu\text{m}$  with a high mass resolution of  $2000\text{ m}/\Delta\text{m}$ . All the samples were treated prior to analysis with exactly the same protocol described elsewhere in Ref. [43] to obtain flat bituminous films of approximately  $1\text{ mm}$ . The spectra for all the samples were analysed based on the intensity of the areas of selective mass-to-charge-ratios, assigned to specific ions (Table 3), normalised by the total recorded ions' intensity (counts). Example spectra of bitumen A of positive and negative ions are given in Fig. 4.

### 2.3.5. Experimental challenges

Although the techniques used in this study are robust enough, limitations may still exist, especially when investigating a multi-component mixture like bitumen. This needs to be acknowledged when reviewing and comparing the findings of each of the techniques as the results may be contradictory.

First of all, FTIR-ATR and TOF-SIMS are in fact both surface analysis methods with different penetration depths, of a maximum of

Table 3

Utilised negative and positive oxygenated ion fragments.

| Ion                               | Observed mass ( $m/z$ ) | Assignment of molecular structure |
|-----------------------------------|-------------------------|-----------------------------------|
| $\text{OH}^-$                     | 17.003                  | $(\text{OH})_x$ -containing       |
| $\text{C}_2\text{OH}^-$           | 41.005                  | $(\text{OH})_x$ -containing       |
| $\text{CHSO}^-$                   | 60.974                  | $\text{SO}_x$ -containing         |
| $\text{C}_2\text{H}_3\text{SO}^-$ | 74.989                  | $\text{SO}_x$ -containing         |
| $\text{C}_6\text{HO}^-$           | 89.001                  | $(\text{OH})_x$ -containing       |
| $\text{C}_3\text{H}_7^+$          | 43.055                  | Aliphatic                         |
| $\text{C}_4\text{H}_7^+$          | 55.054                  | Aliphatic                         |
| $\text{C}_4\text{H}_9^+$          | 57.070                  | Aliphatic                         |
| $\text{C}_5\text{H}_7^+$          | 67.049                  | Aliphatic                         |
| $\text{C}_5\text{H}_9^+$          | 69.068                  | Aliphatic                         |
| $\text{C}_5\text{H}_{11}^+$       | 71.088                  | Aliphatic                         |
| $\text{C}_6\text{H}_9^+$          | 81.065                  | Aliphatic                         |
| $\text{C}_6\text{H}_{11}^+$       | 83.085                  | Aliphatic                         |
| $\text{C}_6\text{H}_{13}^+$       | 85.104                  | Aliphatic                         |
| $\text{C}_7\text{H}_{11}^+$       | 95.079                  | Aliphatic                         |
| $\text{C}_7\text{H}_{13}^+$       | 97.102                  | Aliphatic                         |
| $\text{C}_9\text{H}_7^+$          | 115.033                 | Aromatic                          |
| $\text{C}_{10}\text{H}_8^+$       | 128.036                 | Aromatic                          |
| $\text{C}_{13}\text{H}_9^+$       | 165.035                 | Aromatic                          |

2–3  $\mu\text{m}$  for FTIR-ATR [44], and only a few nanometres for TOF-SIMS [42]. In TOF-SIMS an air-cooled surface is investigated, while in FTIR-ATR, the interface as formed against the ATR diamond crystal is investigated. In literature, it has been demonstrated that bitumen may exhibit a different composition depending on the

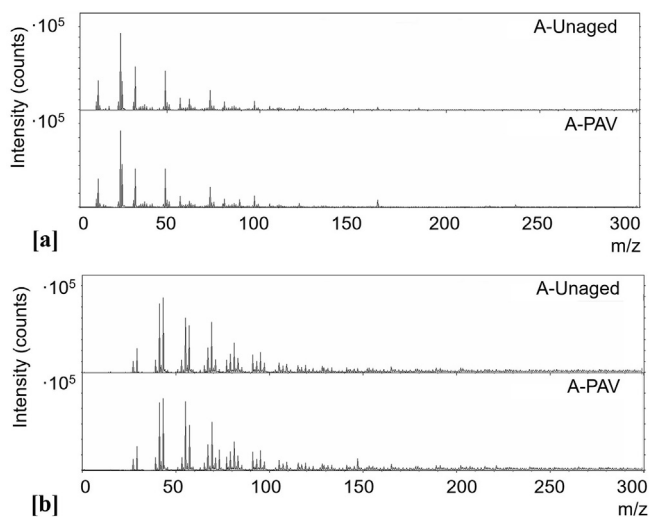


Fig. 4. Example of negative [a] and positive [b] TOF-SIMS ion spectra of bitumen A in the unaged state and after PAV.

substrate and the environment [43,45,46]. Especially, the reproducibility of TOF-SIMS results is an issue that needs special care as the exact film thickness and flatness may affect the obtained spectra. In the current study the preparation procedure, the thermal history of the binders and the control of film thickness was kept constant, with the latter calculated by the exact amount of binder used on the substrate.

Secondly, sample preparation and sample thermal history are different for both the FTIR and TOF-SIMS tests: in FTIR a small hot drop is placed directly onto the crystal and tested. In TOF-SIMS, hot bitumen drops are first placed on a substrate, which is then shortly reheated and air-cooled, to achieve a flat surface. The analysis temperature is much lower in TOF-SIMS compared to the other techniques, which could for example influence the extent of crystallisation of the waxy bitumen compounds. For the  $^1\text{H}$  NMR tests, the bitumen is dissolved in deuterated tetrachloroethane, and although several steps were taken to obtain dissolved samples (*i.e.* a solvent with appropriate solubility, ultrasonic bath and visual inspection), there is still a risk of some undissolved species.

Moreover, the detection sensitivity for various chemical compounds is dependent on the respective technique, *i.e.* FTIR is very sensitive to capture basic oxygenated products (carbonyls and sulfoxides) while it is rather insensitive to changes such as a further aromatisation process [47]. Additionally, in TOF-SIMS only the charged species formed (and not the neutral ones) after a chemical bombardment on the surface are detected. The  $^1\text{H}$  NMR by definition will only capture hydrogenated compounds, while CW EPR shows both bulk and surface paramagnetic centres. The spectral intensity will depend on the time after generation of the radicals and as such centres that are too short living will not be detected in the EPR experiment.

Finally, the ageing tests, which are the standard ageing protocols when investigating bitumen, are not conducted in a closed system; so there is a possibility that volatiles, present or formed during ageing may leave the sample. This effect would be the same for all the analyses performed on the sample after the ageing tests.

### 3. Results and discussion

#### 3.1. FTIR analyses

The indices presented in Eqs. (1)–(4) were determined for the three bitumens under investigation before and after laboratory

short and long-term ageing. The results are consistent with the view that an increase with ageing severity is observed after standardised ageing for the main oxidative indices, namely the sulfoxide and the carbonyl index [48,49]. Figs. 5 and 6 depict the evolution of the two indices and the effect of each ageing state is discussed herein in percentage increase of the virgin state.

A relative comparison of the formation rates is performed in terms of percentage differences. The results of bitumen A for the carbonyl index show an increase of 150.7% and 600.1% after RTFOT and PAV respectively, which indicates a more rapid and steep increase compared to bitumen B (79.2% and 157.5%) which differed only in penetration grade (Fig. 5). The presence of carbonyl groups for these two bitumens in the unaged state can be explained by the acidic nature of the crude oil from which they originated. On the contrary, for bitumen C-Unaged, a negligible initial carbonyl index was obtained based on the same analysis procedure. As such percentage differences are meaningless for bitumen C after RTFOT (with an initial unaged index equal to zero), but an increase in carbonyls after RTFOT ageing is clear. The significant increase of carbonyls is apparent in bitumen C after PAV which increased (484.7%) compared in this case with the index in RTFOT. Therefore, it can be speculated that the cumulative carbonyl formation rate was even faster for bitumen C than A, although a numerical straight-forward comparison of the percentage increase cannot be performed.

A detailed inspection of the initial sulfoxide index for C-Unaged implies that this is significantly higher than for bitumen A and B. Concerning the sulfoxide index the three bitumens show similar percentage increase after RTFOT (A-95.3%, B-91.4% and C-91.9%). The effect of the bitumen type seems to be very small on the sulfoxide formation rate after short-term ageing but after PAV ageing the sulfoxide indices increase more for bitumens A and B (A-218.9%, B-246.0%) compared to the increase of the sulfoxide index of bitumen C (123.1%).

Overall, the bitumen type has little effect on the sulfoxide formation rate but seems to affect the carbonyl formation differently. On the other hand, straight-run bitumens from the same crude show a similar increase of sulfoxide upon ageing in the lab, with hard bitumen A exhibiting a more rapid carbonyl increase compared to bitumen B.

The representative indices for the aromatisation of bitumen were also investigated in this work. In the past, it has been

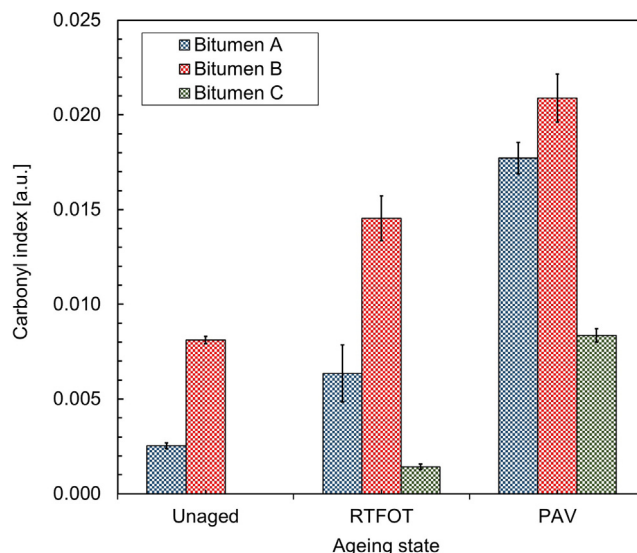


Fig. 5. Evolution of carbonyl index with ageing.



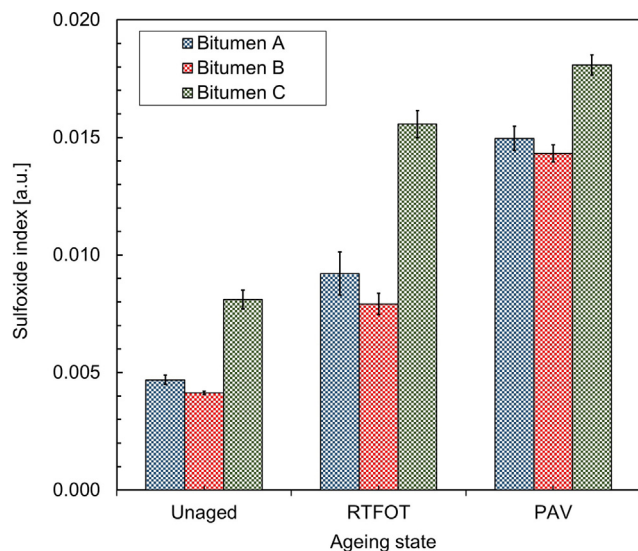


Fig. 6. Evolution of sulfoxide index with ageing.

assumed that aromatisation increases primarily the planarity of perhydroaromatic rings in the fast-rate reaction but it can also cause the aromatisation of alkyl-substituted naphthenic rings during the slow-rate phase [9,50]. Moreover, an interplay between the formation of aromatic structures and a reduction of aliphatics (occurring in a lesser amount) can be hypothesised, which would result in a mutual change of the aromaticity and the branched aliphatic index. Surprisingly in this study, the FTIR indices related to these compounds were constant for both the aromaticity and branched aliphatic index in all the ageing states (Figs. 7 and 8). It was postulated that FTIR was not sensitive enough to capture changes related to aromatisation. Moreover, alcohol regions around  $3200\text{--}3500\text{ cm}^{-1}$ , seem not to be affected by ageing for all the bitumens, whereas an overlap in the C-O stretch of possible alcohol formation could exist with the sulfoxide increase in the FTIR spectra. For that reason, other tests were applied as shown in the next sections.

### 3.2. EPR analyses

The evolution of the organic carbon-centred radicals and the  $\text{VO}^{2+}$  species after routine laboratory ageing simulations is given

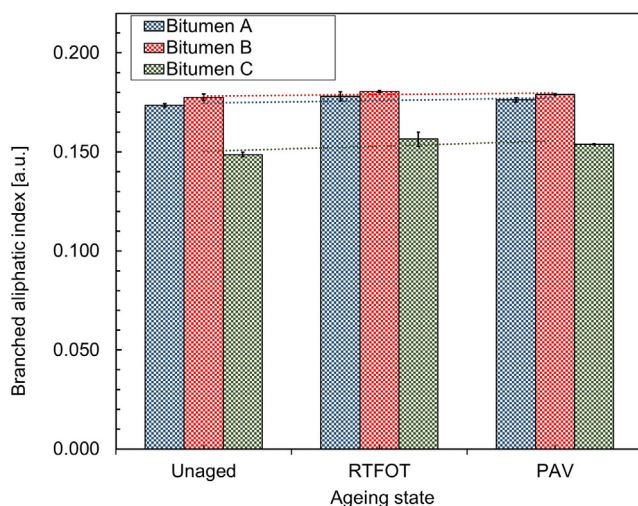


Fig. 7. Branched aliphatic index in all the ageing states.

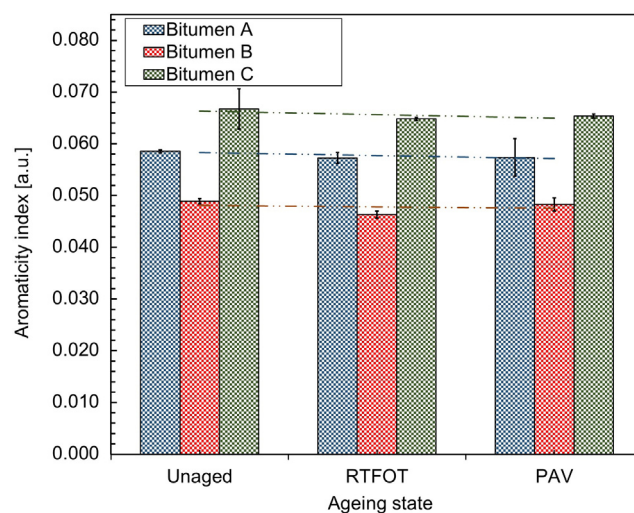


Fig. 8. Aromaticity index in all the ageing states.

in Figs. 9 and 10 respectively. Overall, the carbon-centred organic radicals showed an increase after short term-ageing with RTFOT for all the three bitumens of this work with a significant drop in the number of spins for bitumen C observed upon PAV. Bitumen A and B kept a constant number of spins of carbon-centred organic radicals between short- and long-term ageing. A previous kinetics' study suggested that the oxygen-centred radicals, such as  $\cdot\text{OH}$ , may abstract protons attached to benzyl rings and could yield to carbon-centred radicals [12]. The point at which the plateau of this type of radicals appears is considered as the onset of the slow-rate phase. Hence, the differences of bitumen A, B and C suggest that the intermediate products, such as the organic carbon-based radicals, are affected differently by ageing. Furthermore, the different initial higher number of organic radical spins in bitumen C is possibly related to the visbreaking process of this bitumen.

When it comes to the  $\text{VO}^{2+}$  centres, identified with the EPR analyses, the present study for these metal ions confirms earlier studies [12], namely that these centres remain in general unaffected by the oxidation process, as it is evidenced by the stabilisation of the number of spins in all the ageing states (Fig. 10). The present article raises a significant point about a possible correlation of the vanadyl species and the vanadium content, present in bitumen's composition since it can be exploited as an indicator and marker of the origin following [51].

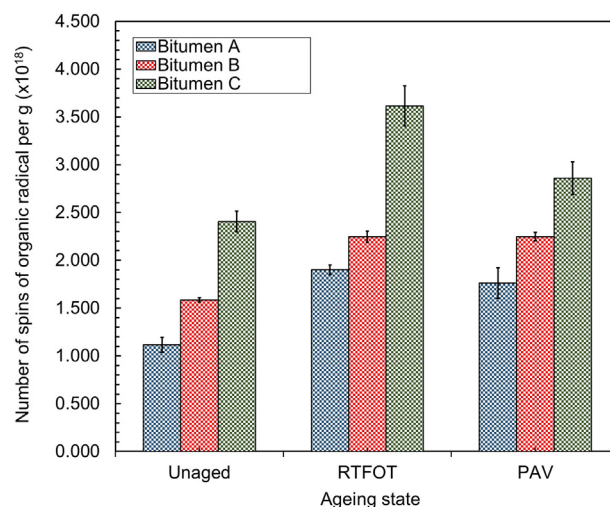


Fig. 9. Evolution of carbon-centred radicals in all the ageing states.

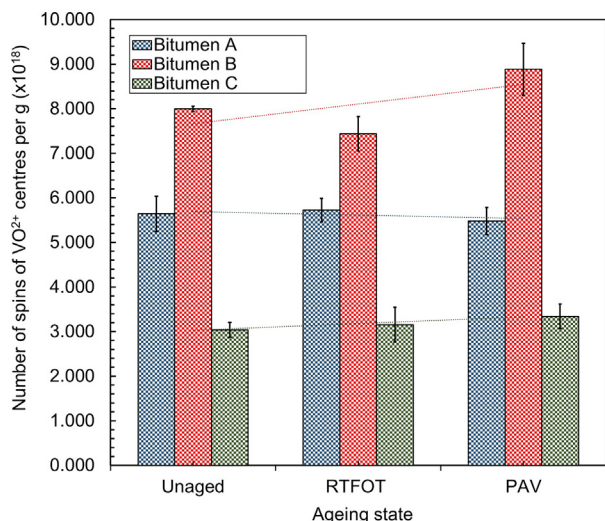


Fig. 10. Evolution of VO<sup>2+</sup> centres in all the ageing states.

Up to this point, the differences between bitumen C and bitumens A and B may affect the initial number of spins of organic radicals in the unaged state. The different penetration grade between bitumen A and B implies also that the distillation grade of the same crude oil may have an effect on the VO<sup>2+</sup> centres with the softer bitumen B presenting the higher number of VO<sup>2+</sup> centres.

### 3.3. <sup>1</sup>H NMR analyses and proton relative distribution

Spectroscopic <sup>1</sup>H NMR analyses were evaluated to gain insights into possible changes of proton distribution upon ageing and thus the chemical composition of bitumens. An inspection of the spectra in all the ageing states for bitumen A (Fig. 3) revealed a large peak at 0.90 ppm assigned to alkyl (methyl) protons and a peak at 1.28 ppm related to alkyl (methylene) protons, something which was observed also for binders B and C. After long term-ageing with PAV, bitumen A showed a peak around 1.67 ppm ascribed to alkyl (methine) protons. The same peak was observed already for B-RTFOT and C-RTFOT with the intensity of the peak increasing after PAV. The broader peak between 2.00 and 2.30 ppm can be assigned to protons on C<sub>α</sub> next to carbonyl and the peak at 2.30 ppm can be assigned to a benzylic proton. No significant peaks were observed in the olefinic proton region (4.00–6.00 ppm) in any of the ageing states. The broader signal from 6.50 to 8.50 ppm is related to the aromatic protons.

Although spectral peaks appear somewhat similar apart from the prominent peak at 1.67 ppm upon ageing, integration of specific regions given in Table 2 (for which relative percentage distribution was determined) allows for the discussion of the chemical alterations upon standardised ageing. The relative occurrence of protons in different chemical environments/ageing states is given in Fig. 11. All the analysed samples present a negligible presence of olefinic protons independent of the bitumen's ageing state. For clarity the standard deviations of this specific region are not presented, whereas standard deviations of all the other regions are included in Fig. 11. In bitumens A and B, the governing region seems to be the methylene, followed by methyl, α-alkyl and aromatic proton regions, while for bitumen C the methyl and α-alkyl region appeared in different decreasing percentage order. The main differences between bitumen A and B are the lower methyl region and the higher methylene region for bitumen A. Since methylene is the region that contributes predominantly in the total spectral region of the aliphatic protons (=H<sub>methylene</sub> + H<sub>methyl</sub> + H<sub>α-alkyl</sub>) its lower percentage for bitumen B is reasonable based on the different distillation grade of the two bitumens. As mentioned previously in the limitations of each spectroscopic technique, <sup>1</sup>H NMR can capture only molecules containing protons, and this should always be taken into account when fractionation is considered as with this technique the total bitumen composition is missing. In addition, bitumens A and B differ from bitumen C mainly by the lower fraction in the aromatic and the higher fraction in the methyl regions.

The effect of the ageing state with regard to the relative percentage of protons was also assessed and presented in Fig. 11. More specifically, in the hard bitumen A, the methylene proton region appears to increase slightly from 59.0% in A-Unaged to 59.5% in A-RTFOT and remains constant in A-PAV (59.6%). The aromatic protons follow the opposite trend (6.0% for A-Unaged to 5.5% for A-PAV). The region linked with the methyl protons fluctuated for bitumen A (19.3% – A-Unaged, 19.8% – A-RTFOT, 19.1% – A-PAV).

Bitumen B originating from the same crude oil presents a similar relative percentage proton distribution after laboratory short- and long-term ageing. It is interesting that the α-alkyl proton zone from 16.0% in B-Unaged decreased in B-RTFOT (13.2%) and PAV (14.2%) compared to the unaged state. A fluctuation for the methyl protons was observed for bitumen B (increased percentage after RTFOT and decreased percentage values upon PAV), a trend which was observed also for bitumen A. Changes in the methylene proton region showed also an upward relative percentage trend with ageing.

Bitumen C, which gave the most apparent difference in the FTIR and the EPR results, showed a different initial proton relative

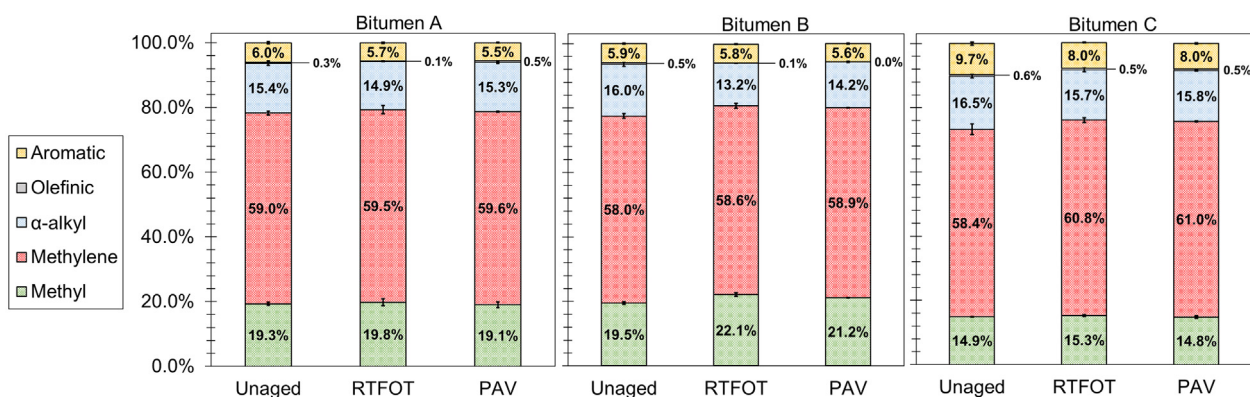


Fig. 11. Percentage distribution of protons in different ageing states of bitumen A, B and C as determined by <sup>1</sup>H NMR.

percentage distribution compared to A and B-Unaged (higher aromatic and  $\alpha$ -alkyl proton percentages, lower methyl proton percentages) but demonstrated, in general, the same trends with ageing. More specifically, bitumen C showed a decreasing trend after short-term ageing with RTFOT for the  $\alpha$ -alkyl proton region shifting respectively from 16.5% in the C-Unaged to 15.7% in C-RTFOT and in 15.8% in the C-PAV, something which was observed also for bitumen B. Similar to bitumens A and B, increasing trends in the methylene and methyl proton regions of bitumen C was also observed, with the methyl proton region increasing with RTFOT ageing. The aromatic region appeared to decrease with ageing for bitumen C.

Obstacles of exploratory studies to identify chemical differences upon ageing were overcome by grouping the main proton categories, acknowledging always the limitations that may exist for the application of this technique to bitumen. Therefore, bitumen A and B exhibited in general similar relative percentage distribution of protons as expected for the same crude oil in the unaged state but also upon laboratory ageing where the percentage distribution of protons was quite similar. In addition, the formation of polycyclic aromatics due to the aromatisation process is not expected to be captured with  $^1\text{H}$  NMR since they do not contain a hydrogen in the middle and the relative decrease of this region for bitumen A and C can be possibly attributed to the risk of precipitation due to aromatics condensation with ageing.

### 3.4. TOF-SIMS oxygenated fragments

Molecular investigation of the oxygenated products after the combined effect of short- and long-term ageing was conducted with TOF-SIMS on the surface of the three bituminous samples. Ageing may affect the compatibility of the wax present in bitumen C to appear more pronounced upon ageing in the surface of the films. Although clear differences cannot be seen between the different ageing states *i.e.* in the spectra of bitumen A (Fig. 4), a thorough inspection of certain fragment ions assisted to form a more clear view for the products.  $m/z$  values in the negative ion spectra of all the bituminous tested samples were classified in groups of ion fragments with generic formulas  $\text{RSO}_x$  and  $\text{RHO}_x$  given in Table 3. Selected  $m/z$  values in the positive ion spectra were assigned to aromatic and aliphatic ion fragments (Table 3).

The findings of the  $(\text{OH})_x$ -containing fragments of bitumen A and B and partially for bitumen C point out that other products such as alcohols/ethers or carboxylic acids can be formed. This is evident by the higher intensity of most of the  $(\text{OH})_x$ -containing fragments (attributed possibly to alcohols) after PAV compared to the unaged state which was not observed for specific ion fragments ( $\text{C}_2\text{OH}^-$ ,  $\text{C}_6\text{OH}^-$ ) of bitumen C (Fig. 12), most probably as a result of the prominent presence of wax in its surface.

Similar trends follow for the increase of the ion fragments with generic formula  $\text{RSO}_x$  given in Fig. 13. The results of bitumen A and B support the formation of considerable amounts of sulfoxide-containing compounds after the sequential short and long-term ageing as the intensities of A-PAV and B-PAV remain higher than the unaged state. Caution should always be taken concerning the specific sulfoxide-containing fragments observed with TOF-SIMS which give a partial view of the total sulfoxides present in bitumen which FTIR might capture in a greater penetration depth; this means that limitations should be again acknowledged when comparing the different techniques. Potentially, the results of the two surface techniques could be used to exploit the surface effects of oxidation in bituminous films. Bitumen C seems to reduce the sulfoxide-containing ion fragments with ageing something which does not agree with the FTIR results. This may be explained by the segregation of wax, present in this bitumen, on the surface of

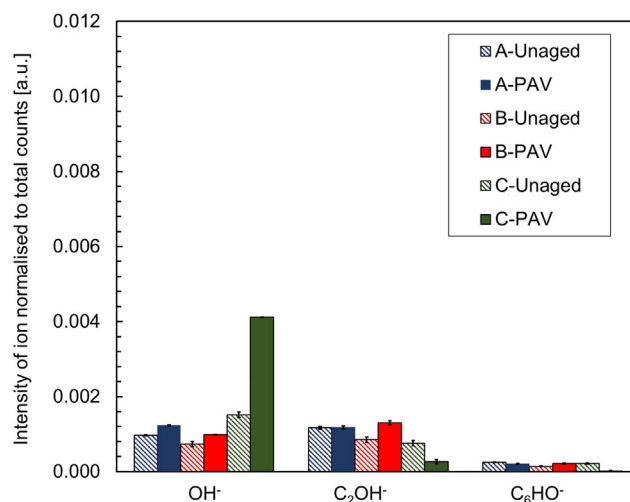


Fig. 12. Intensity of  $(\text{OH})_x$ -containing compounds in all the ageing states.

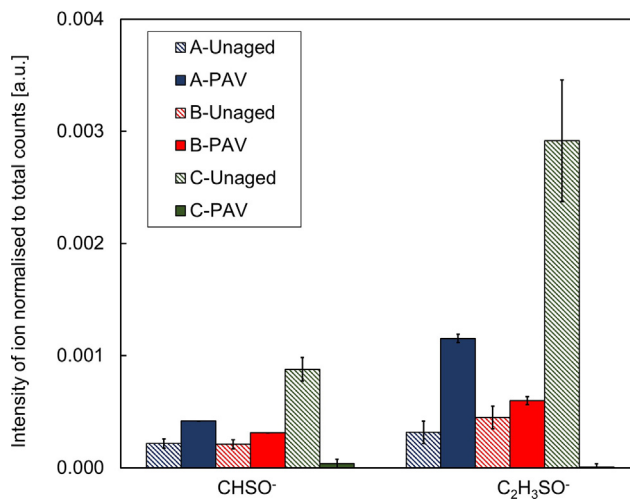


Fig. 13. Intensity of  $\text{SO}_x$ -containing compounds in all the ageing states.

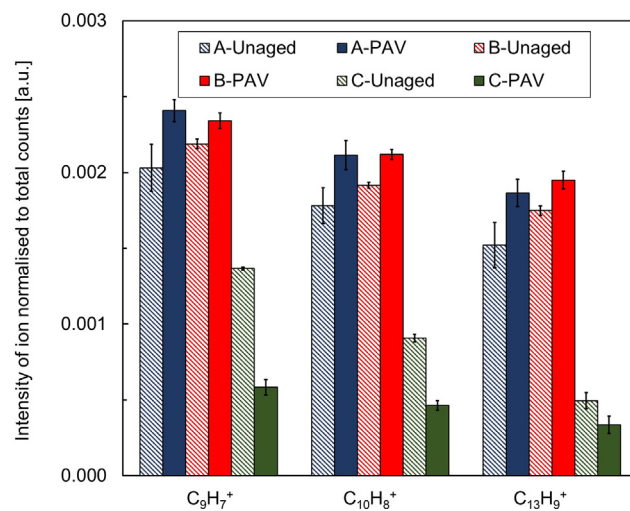


Fig. 14. Intensity of PAH fragments in all the ageing states.

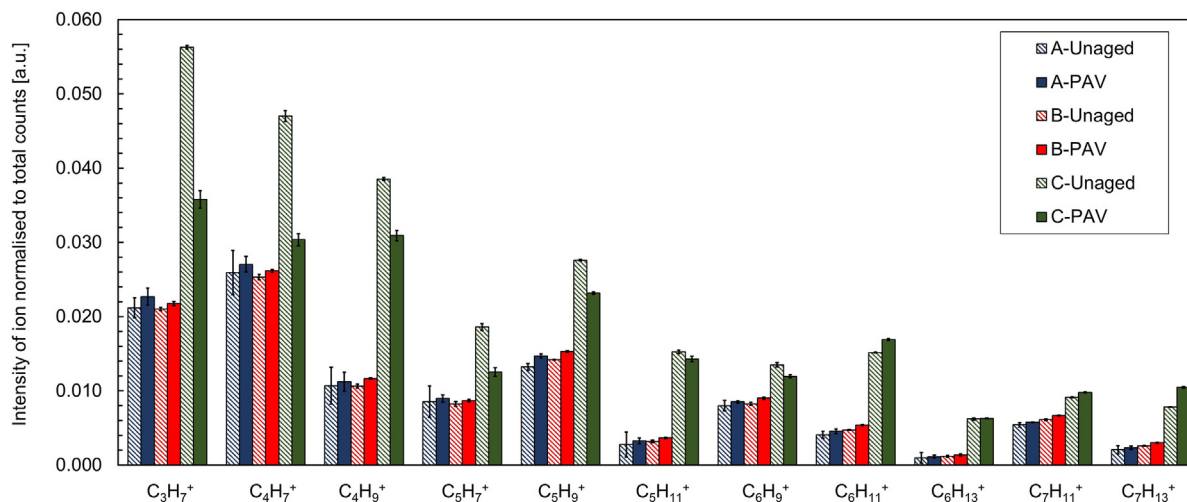


Fig. 15. Intensity of aliphatic fragments in all the ageing states.

the bituminous film, resulting in aliphatic compounds which cover most of the surface [12,52].

The analysis of selected ions in the positive ion spectra (Fig. 14) assigned to polycyclic aromatics hydrocarbons (PAH) is also discussed. The intensity of PAHs of B-Unaged and A-Unaged increased slightly after PAV, whereas a significant drop of PAHs with ageing for bitumen C was captured, probably due to the increase of the waxy particles on the surface upon ageing. Finally, bitumens A and B showed an almost constant behaviour (or a slight increase) of aliphatic ion fragments upon PAV in contrary to bitumen C which showed a decrease for specific aliphatic ion fragments (Fig. 15). The intensity of the aliphatics for bitumen C appeared the highest a fact that can be explained by the wax present in this binder and the association of wax-related particles with aliphatics on the surface of this bitumen.

#### 4. Conclusions

This study addressed the main chemical changes that take place in bitumen with standardised laboratory short- and long-term ageing based on advanced spectroscopic techniques. Three binders were investigated, bitumen A and B originating from the same crude source, while bitumen C was obtained from a different source, by a different manufacturing process, and contained natural wax.

FTIR supported, in agreement with past literature, the increase of the oxygenated indices of sulfoxide and carbonyl for all binders, independently of bitumen source, distillation process and performance for all the ageing steps. Differences in the extent of carbonyl and sulfoxide formation were observed between the various binders. In FTIR, no clear changes appeared for the aromaticity and branched aliphatic indices with the applied FTIR analysis method. To understand further the formation of the final products, EPR analyses explored the role of organic carbon-centred radicals. These were increased for all three bitumens of different crude source, distillation and empirical properties with short-term ageing and stabilised onwards for the wax-free bitumen A and B, while they slightly decreased for the waxy, visbroken bitumen C. The EPR VO<sup>2+</sup> centres remained relatively constant and were almost insensitive to ageing for all three bitumens, regardless of their crude source or distillation. Additionally, <sup>1</sup>H NMR results showed that the relative distribution of protons is rather unaffected by the ageing steps. Only slight changes were observed, such as an increase in the relative amount of methyl and methylene protons, and a decrease in  $\alpha$ -alkyl and aromatic protons. TOF-SIMS managed to

reveal a more detailed view of the increase of sulfoxide-containing compounds which were increased significantly after the sequentially short- and long-term ageing for bitumens A and B originating from the same crude source and varying only in empirical properties. For the waxy, visbroken bitumen C originating from a different crude source, the presence of wax affected the surface molecular characterisation reporting a decrease for most of the SO<sub>x</sub>- and (OH)<sub>x</sub>-containing fragments. The (OH)<sub>x</sub>-containing fragments suggested that apart from carbonyls, other products such as alcohols and carboxylic acids can be produced.

Since each technique has its specific limitations, the results from different techniques may sometimes seem conflicting and should be interpreted carefully. Moreover, some of the test methods are typical surface/interface techniques with different penetration depths, such as TOF-SIMS and FTIR, while for others, *i.e.* liquid <sup>1</sup>H NMR, the sample needs to be dissolved in a solvent. These different parameters may have an effect on the results.

In summary, this work reported the oxygenated intermediate and final products in bitumen and provided some experimental insights in order to understand better the oxidative mechanisms that could occur in bitumen besides the well-reported sulfoxide and carbonyl formation. In the future, a comparison between the ageing mechanisms of bitumen after laboratory ageing with the mechanisms of field aged bitumen is proposed to be performed in order to understand whether similar changes in bitumen chemistry take place in field conditions.

#### CRedit authorship contribution statement

**Georgios Pipintakos:** Methodology, Investigation, Validation, Software, Formal analysis, Writing - original draft. **Hilde Soenen:** Conceptualization, Supervision, Writing - review & editing. **H.Y. Vincent Ching:** Software, Formal analysis, Investigation, Validation, Writing - review & editing. **Christophe Vande Velde:** Software, Formal analysis, Investigation, Writing - review & editing. **Sabine Van Doorslaer:** Conceptualization, Writing - review & editing. **Filip Lemière:** Formal analysis, Writing - review & editing. **Aikaterini Varveri:** Writing - review & editing. **Wim Van den bergh:** Conceptualization, Supervision, Writing - review & editing.

#### Declaration of Competing Interest

The authors declare that they have no known competing financial interests or personal relationships that could have appeared to influence the work reported in this paper.

## Acknowledgements

The authors gratefully acknowledge the technical assistance by Jimmy Matheussen from Bureau Veritas, Pieter Mampuy (ORSY) and Glenn Van Haesendonck (BAMS) from the University of Antwerp, as well as support from Nynas AB and the European Union for H.Y. Vincent Ching's H2020-MSCA-IF grant (grant number 792946. iSPY).

## References

- J.S. Moulthrop, M. Massoud, The SHRP Materials Reference Library, Washington DC, 1993.
- P.E.Y. Wang, Y. Wen, K. Zhao, D. Chong, A.S.T. Wong, Evolution and locational variation of asphalt binder aging in long-life hot-mix asphalt pavements, *Constr. Build. Mater.* 68 (2014) 172–182, <https://doi.org/10.1016/j.conbuildmat.2014.05.091>.
- F. Wang, Y. Xiao, P. Cui, J. Lin, M. Li, Z. Chen, Correlation of asphalt performance indicators and aging degrees: a review, *Constr. Build. Mater.* 250 (2020), <https://doi.org/10.1016/j.conbuildmat.2020.118824> 118824.
- X. Lu, U. Isacson, Effect of ageing on bitumen chemistry and rheology, *Constr. Build. Mater.* 16 (2002) 15–22, [https://doi.org/10.1016/S0950-0618\(01\)00033-2](https://doi.org/10.1016/S0950-0618(01)00033-2).
- M.C. Cavalli, M. Zauamanis, E. Mazza, M.N. Partl, L.D. Poulikakos, Aging effect on rheology and cracking behaviour of reclaimed binder with bio-based rejuvenators, *J. Clean. Prod.* 189 (2018) 88–97, <https://doi.org/10.1016/j.jclepro.2018.03.305>.
- J.C. Petersen, R. Glaser, Asphalt oxidation mechanisms and the role of oxidation products on age hardening revisited, *Road Mater. Pavement Des.* 12 (2011) 795–819, <https://doi.org/10.1080/14680629.2011.9713895>.
- X. Hou, F. Xiao, J. Wang, S. Amirkhanian, Identification of asphalt aging characterization by spectrophotometry technique, *Fuel* 226 (2018) 230–239, <https://doi.org/10.1016/j.fuel.2018.04.030>.
- A.A.A. Molenaar, E.T. Hagos, M.F.C. van de Ven, Effects of aging on the mechanical characteristics of bituminous binders in PAC, *J. Mater. Civ. Eng.* 22 (2010) 779–787, [https://doi.org/10.1061/\(ASCE\)MT.1943-5533.0000021](https://doi.org/10.1061/(ASCE)MT.1943-5533.0000021).
- J.C. Petersen, A review of the fundamentals of asphalt oxidation (E-C140), *Transp. Res. Rec. J. Transp. Res. Board* (2009), <https://doi.org/10.17226/23002>.
- The Shell Bitumen Handbook, sixth ed., ICE Publishing, 2015. <https://doi.org/10.1680/tsbh.58378>.
- L. Loebera, G. Muller, J. Morel, O.C. Sutton, L. Havre, L. Havre, Bitumen in colloid science : a chemical , structural and rheological approach 77 (1998) 1443–1450.
- G. Pipintakos, H.Y.V. Ching, H. Soenen, P. Sjövall, U. Mühlich, S. Van Doorslaer, A. Varveri, W. Van den bergh, X. Lu, Experimental investigation of the oxidative ageing mechanisms in bitumen, *Constr. Build. Mater.* 260 (2020) 119702, <https://doi.org/10.1016/j.conbuildmat.2020.119702>.
- P. Herrington, B. James, T.F.P. Henning, Validation of a bitumen oxidation rate model, *Transp. Res. Rec. J. Transp. Res. Board* 2632 (2017) 110–118, <https://doi.org/10.3141/2632-12>.
- U. Mühlich, G. Pipintakos, C. Tsakalidis, Mechanism based diffusion-reaction modelling for predicting the influence of SARA composition and ageing stage on spurt completion time and diffusivity in bitumen 267 (2021). <https://doi.org/10.1016/j.conbuildmat.2020.120592>.
- J. Petersen, P. Harnsberger, Asphalt aging: dual oxidation mechanism and its interrelationships with asphalt composition and oxidative age hardening, *Transp. Res. Rec. J. Transp. Res. Board* 1638 (1998) 47–55, <https://doi.org/10.3141/1638-06>.
- P.R. Herrington, Thermal decomposition of asphalt sulfoxides, *Fuel* 74 (1995) 1232–1235.
- J.C. Petersen, R.E. Robertson, J.F. Branthaver, P.M. Harnsberger, J.J. Duvall, S.S. Kim, D.A. Anderson, D.W. Christiansen, H.U. Bahia, R. Dongre, Binder characterization and evaluation. Volume 4: Test methods, 1994.
- L.D. Poulikakos, A. Cannone Falchetto, D. Wang, L. Porot, B. Hofko, Impact of asphalt aging temperature on chemomechanics, *RSC Adv.* 9 (2019) 11602–11613, <https://doi.org/10.1039/C9RA00645A>.
- B. Hofko, L. Porot, A.F. Cannone, L. Poulikakos, L. Huber, X. Lu, H. Grothe, K. Mollenhauer, FTIR spectral analysis of bituminous binders: reproducibility and impact of ageing temperature, *Mater. Struct.* 51 (2018), <https://doi.org/10.1617/s11527-018-1170-7>.
- D. Lesueur, A. Teixeira, M.M. Lázaro, D. Andaluz, A. Ruiz, A simple test method in order to assess the effect of mineral fillers on bitumen ageing, *Constr. Build. Mater.* 117 (2016) 182–189, <https://doi.org/10.1016/j.conbuildmat.2016.05.003>.
- EN12607-1: Bitumen and Bituminous Binders, Determination of the Resistance to Hardening Under the Influence of Heat and Air–Part 1: RTFOT Method, 2007.
- EN 14769: Bitumen and Bituminous Binders, Accelerated Long-term Ageing Conditioning by a Pressure Ageing Vessel (PAV), 2012.
- K. Zhao, Y. Wang, F. Li, Influence of ageing conditions on the chemical property changes of asphalt binders, *Road Mater. Pavement Des.* (2021) 1–29, <https://doi.org/10.1080/14680629.2019.1637771>.
- F. Liu, Z. Zhou, X. Zhang, Y. Wang, On the linking of the rheological properties of asphalt binders exposed to oven aging and PAV aging, *Int. J. Pavement Eng.* (2019) 1–10, <https://doi.org/10.1080/10298436.2019.1608992>.
- N.A. Al-azri, S.H. Jung, K.M. Lunsford, A. Ferry, J.A. Bullin, R.R. Davison, C.J. Glover, Binder oxidative aging in Texas pavements hardening rates, hardening susceptibilities, and impact of pavement depth (n.d.) 12–20.
- C.H. Domke, R.R. Davison, C.J. Glover, Effect of oxygen pressure on asphalt oxidation kinetics RT (2000) 592–598. <https://doi.org/10.1021/ie9906215>.
- Y. Li, S. Wu, Q. Liu, Y. Dai, C. Li, H. Li, S. Nie, Aging degradation of asphalt binder by narrow-band UV radiations with a range of dominant wavelengths, *Constr. Build. Mater.* 220 (2019) 637–650, <https://doi.org/10.1016/j.conbuildmat.2019.06.035>.
- J. Mirwald, D. Maschauer, B. Hofko, H. Grothe, Impact of reactive oxygen species on bitumen aging – the Viennese binder aging method, *Constr. Build. Mater.* 257 (2020) 119495, <https://doi.org/10.1016/j.conbuildmat.2020.119495>.
- P.R. Herrington, Diffusion and reaction of oxygen in bitumen films, *Fuel* 94 (2012) 86–92, <https://doi.org/10.1016/j.fuel.2011.12.021>.
- A. Dony, L. Ziyani, I. Drouadaine, S. Pouget, S. Faucon-Dumont, D. Simard, V. Mouillet, J.E. Poirier, T. Gabet, L. Boulange, A. Nicolai, C. Gueit, 1, MURE National Project : FTIR spectroscopy study to assess ageing of asphalt mixtures, in: 6th Eurasphalt Eurobitume Congr., 2016, <https://doi.org/10.14311/EE.2016.154>.
- R. Tauste, Understanding the bitumen ageing phenomenon: a review, *Constr. Build. Mater.* 192 (2018) 593–609, <https://doi.org/10.1016/j.conbuildmat.2018.10.169>.
- F.J. Ortega, F.J. Navarro, M. Jasso, L. Zanzotto, Physicochemical softening of a bituminous binder by a reactive surfactant (dodecyl succinic anhydride, DSA), *Constr. Build. Mater.* 222 (2019) 766–775, <https://doi.org/10.1016/j.conbuildmat.2019.06.117>.
- J. Lamontagne, P. Dumas, V. Mouillet, J. Kister, Comparison by Fourier transform infrared (FTIR) spectroscopy of different ageing techniques: application to road bitumens, *Fuel* 80 (2001) 483–488, [https://doi.org/10.1016/S0016-2361\(00\)00121-6](https://doi.org/10.1016/S0016-2361(00)00121-6).
- A. Stoll, S. Schweiger, EasySpin, a comprehensive software package for spectral simulation and analysis in EPR, *J. Magn. Reson.* 178 (2006) 42–55, <https://doi.org/10.1016/j.jmr.2005.08.013>.
- M. Espinosa, P.A. Camper, R. Salcedo, Electron spin resonance and electronic structure of vanadyl–porphyrin in heavy crude oils, *Inorg. Chem.* 40 (2001) 4543–4549, <https://doi.org/10.1021/ic000160b>.
- L.G. Gilinskaya, EPR spectra of V(IV) complexes and the structure of oil porphyrins, *J. Struct. Chem.* 49 (2008) 245–254, <https://doi.org/10.1007/s10947-008-0120-6>.
- Vasanth Ramachandran, Johan van Tol, Amy M. McKenna, Ryan P. Rodgers, Alan G. Marshall, Naresh S. Dalal, High field electron paramagnetic resonance characterization of electronic and structural environments for paramagnetic metal ions and organic free radicals in deepwater horizon oil spill tar balls, *Anal. Chem.* 87 (2015) 2306–2313, <https://doi.org/10.1021/ac504080g>.
- N. Nciri, N. Kim, N. Cho, Chemical characterization of gilsonite bitumen chemical characterization of gilsonite, *Bitumen* (2014), <https://doi.org/10.4172/2157-7463.1000193>.
- J.C. Poveda, D.R. Molina, Average molecular parameters of heavy crude oils and their fractions using NMR spectroscopy, *J. Pet. Sci. Eng.* 84–85 (2012) 1–7, <https://doi.org/10.1016/j.petrol.2012.01.005>.
- L.J. O'Neil, P.E. Heckelman, C.B. Koch, K.J. Roman, *The Merck Index, an Encyclopedia of Chemicals, Drugs, and Biologicals*, 14th ed., Merck Research Laboratories, 2006.
- C.O. Rossi, P. Caputo, G. De Luca, L. Maiuolo, S. Eskandarsefat, C. Sangiorgi, 1H-NMR spectroscopy: a possible approach to advanced bitumen characterization for industrial and paving applications, *Appl. Sci.* 8 (2018), <https://doi.org/10.3390/app8020229>.
- V. Thiel, P. Sjövall, Time-of-flight secondary ion mass spectrometry (TOF-SIMS): principles and practice in the biogeosciences, in: *Princ. Pract. Anal. Tech. Geosci.*, Royal Society of Chemistry, 2015, pp. 122–170.
- X. Lu, P. Sjövall, H. Soenen, Structural and chemical analysis of bitumen using time-of-flight secondary ion mass spectrometry (TOF-SIMS), *Fuel* 199 (2017) 206–218, <https://doi.org/10.1016/j.fuel.2017.02.090>.
- A.M. Hung, A. Goodwin, E.H. Fini, Effects of water exposure on bitumen surface microstructure, *Constr. Build. Mater.* 135 (2017) 682–688, <https://doi.org/10.1016/j.conbuildmat.2017.01.002>.
- J. Blom, H. Soenen, A. Katsiki, N. Van Den Brande, H. Rahier, Investigation of the bulk and surface microstructure of bitumen by atomic force microscopy, *Constr. Build. Mater.* 177 (2018) 158–169, <https://doi.org/10.1016/j.conbuildmat.2018.05.062>.
- A. Ramm, M.C. Downer, N. Sakib, A. Bhasin, Morphology and kinetics of asphalt binder microstructure at gas, liquid and solid interfaces, *J. Microsc.* 276 (2019) 109–117, <https://doi.org/10.1111/jmi.v276.310.1111/jmi.12842>.
- H. Soenen, X. Lu, O.-V. Laukkanen, Oxidation of bitumen: molecular characterization and influence on rheological properties, *Rheol. Acta* 55 (2016) 315–326, <https://doi.org/10.1007/s00397-016-0919-6>.

- [48] G. Tarsi, A. Varveri, C. Lantieri, A. Scarpas, C. Sangiorgi, Effects of different aging methods on chemical and rheological properties of bitumen, *J. Mater. Civ. Eng.* 30 (2018), [https://doi.org/10.1061/\(ASCE\)MT.1943-5533.0002206](https://doi.org/10.1061/(ASCE)MT.1943-5533.0002206).
- [49] I. Gabrielle do Nascimento Camargo, B. Hofko, J. Mirwald, G. Hinrich, Effect of thermal and oxidative aging on asphalt binders rheology and chemical composition, *Materials (Basel)* 13 (2020) 4438, <https://doi.org/10.3390/ma13194438>.
- [50] J.F. Branham, J.C. Petersen, R.E. Robertson, J.J. Duvall, S.S. Kim, P.M. Harnsberger, T. Mill, E.K. Ensley, F.A. Barbour, J.F. Schabron, SHRP-A-368 Binder Characterization and Evaluation Volume 2 : Chemistry, Washington, DC, 1993.
- [51] J.H. Tannous, A. de Klerk, Quantification of the free radical content of oilsands bitumen fractions, *Energy Fuels* 33 (2019) 7083–7093, <https://doi.org/10.1021/acs.energyfuels.9b01115>.
- [52] X. Lu, P. Sjövall, H. Soenen, M. Andersson, Microstructures of bitumen observed by environmental scanning electron microscopy (ESEM) and chemical analysis using time-of-flight secondary ion mass spectrometry (TOF-SIMS), *Fuel* 229 (2018) 198–208, <https://doi.org/10.1016/j.fuel.2018.05.036>.